Online Data Supplement

Plasmalemmal Vesicle Associated Protein (PV1) in Caveolae Controls Lung Endothelial Permeability

Joshua H. Jones[1,2], Emily Friedrich[1], Zhigang Hong[1], Richard D. Minshall[1,3,4], Asrar B. Malik[1,3]

Author affiliations:

[1]Department of Pharmacology, [2]Medical Scientist Training Program, [3]Center for Lung and Vascular Biology, and [4]Department of Anesthesiology, College of Medicine, University of Illinois, Chicago, Illinois

Extended Methods, Figures and Tables

Mice

Animals were bred and maintained in a pathogen-free setting at the University of Illinois at Chicago following approval by the Institutional Animal Care and Use Committee. C57BL/6J mice were purchased from Jackson Laboratory (#000664). $PV1^{fl/fl}$ mice (provided by Dr. Radu Stan) (1) were crossed with endothelial Cdh5-CreERT2 mice (provided by Dr. Ralf Adams), which upon tamoxifen delivery will activate Cre recombinase activity specifically in endothelial cells. Tamoxifen (Sigma #T5648) was dissolved in corn oil (10 mg/ml) and delivered via intraperitoneal injection daily for five consecutive days. Mice were allowed to rest for two or four weeks prior to experimentation.

Measurement of pulmonary vessel filtration coefficient

Mice were anesthetized with ketamine (100 mg/kg body weight) and xylazine (15 mg/kg body weight) via intraperitoneal injection. The pulmonary artery and left atrium were subsequently cannulated. Lungs and heart were extracted and suspended from a counter-weighted beam balance. Lung weight gain was measured after a step increase (10 cm_{H20}) in venous pressure for 20 minutes. The rate of the lung weight gain was normalized to the lung dry weight and pressure change, thus providing the microvascular filtration coefficient (milliliters x min^{-1} x cmH_20 x g dry $weight^{-1}$).

Evans blue-albumin and Albumin PS measurements

Evans Blue-Albumin (Sigma #E2129, 25 mg/kg) or radiolabeled albumin (1 microcurie;^{125}I albumin, AnazaoHealth) was injected into anesthetized mice and allowed to circulate in the bloodstream for 30 minutes. Mouse lungs were subsequently perfused via the right ventricle with DPBS (Gibco #14190144) for 2 minutes. Mouse lungs exposed to EBA were extracted,

weighed, and subsequently homogenized in 1 mL of DPBS. Homogenized samples were combined with 2 mL of formamide and placed at 60 degrees Celsius for 24 hours. Evans blue dye concentration in supernatants was measured spectrophotometrically at absorbance of 620 and 740 nm. For mice exposed to radiolabeled albumin, blood was withdrawn from the inferior vena cava prior to lung perfusion. Radioactivity was subsequently counted in the indicated organs and blood samples. Organs were subsequently placed in a 60 degrees Celsius incubator for at least 48 hours, weighed, and measurements were used for Albumin PS calculations.

Wet-to-Dry Lung Weight Ratio

Mice were anesthetized with ketamine (100 mg/kg body weight) and xylazine (15 mg/kg body weight) via intraperitoneal injection. The thoracic and abdominal cavities were exposed, organs were removed, weighed in pre-weighed tubes, and incubated at 60 degrees Celsius for 7 days. Organs were removed and re-weighed, with calculations subsequently performed to divide the recorded wet mass by the dry mass.

Extravascular Lung Water Measurements

Mice were anesthetized with ketamine (100 mg/kg body weight) and xylazine (15 mg/kg body weight) via intraperitoneal injection. The thoracic and abdominal cavities were exposed, and a blood sample was withdrawn (150-200 μl) from the inferior vena cava. The lungs were removed from the thoracic cavity and placed into a pre-weighed tube, weighed, and homogenized in 1 mL of de-ionized water. Samples were re-weighed, and 250 mL of homogenate was removed and centrifuged at 13000 x g for 10 minutes. Aliquots (12 μl) of lung homogenate supernatant and the blood sample were assessed for hematocrit and hemoglobin concentration (Hemocue Hb 201 analyzer). The remainder (~150 μl) of lung homogenate, lung supernatant, and blood sample were aliquoted onto pre-weighed aluminum dishes, weighed,

and stored at 60 degrees Celsius for at least 24 hours. Dry samples were removed and re-weighed. ELW measurements were calculated using previously described formulas (2).

Transmission Electron Microscopy

Colloidal gold-albumin (Au-Albumin) tracer was prepared as previously described (3). Briefly, mice were anesthetized followed by cannulation of the pulmonary artery and left atrium. Lungs were first perfused with HBSS (Gibco #14025092) for 5 minutes. Colloidal gold albumin tracer solution was subsequently perfused into the lung and collected from the left atrium for a period of 15 minutes. Lungs were washed with HBSS for 5 minutes, fixed via perfusion with 2.5% glutaraldehyde, 4% PFA, 0.1 M HEPES and 2 mM $CaCl_2$. Lungs were minced into 1 mm pieces and subsequently fixed as previously described (3).

Endotoxin Challenge

To analyze the effects of endotoxin-induced lung damage on PV1 expression, we exposed WT mice (C57BL6J) aged 8-10 weeks were exposed to nebulized saline or *Escherichia coli* LPS (Sigma #L2880, 1 mg/ml) for one hour each day for four consecutive days. At the indicated time points (day 0, day 4, and day 7), mice were sacrificed, and lungs were removed for downstream qPCR or Western Blot analysis.

Blood Counts, Ascites and Serum Chemistry Analysis

Mice were anesthetized with ketamine (100 mg/kg body weight) and xylazine (15 mg/kg body weight) via intraperitoneal injection. The thoracic cavities were exposed, and a blood sample was withdrawn (150-200 μl) from the inferior vena cava. In *PV1*$^{i\Delta EC}$ mice, ascites fluid was withdrawn from the abdominal cavity prior to blood sample withdrawal. Blood and ascites fluid samples were analyzed at the Biologic Resources Laboratory at UIC.

Quantitative Real-Time PCR

Freshly isolated lungs were homogenized in Trizol Reagent (Invitrogen, #15596026), allowed to rest at room temperature for five minutes, and centrifuged at 12,000 x g for five minutes at 4 degrees Celsius. The supernatant was removed and placed in a new 1.5 mL centrifuge tube. 200 mL chloroform was added to the supernatant, mixed vigorously for 15 seconds, and incubated at room temperature for 3 minutes. The mixture was subsequently centrifuged at 12,000 x g for 15 minutes at 4 degrees Celsius. The resulting upper phase of the mixture was separated into a new tube and used for further experiments using the RNA Mini Kit (Qiagen, #74104) per manufacturer's protocol.

Cultured endothelial cells were rinsed twice with DPBS (without calcium or magnesium) and lysed with Buffer RLT. An equal volume of 70% alcohol was added to the sample and processed using the RNA Mini Kit (Qiagen, #74104) per manufacturer's protocol. RNA concentration was measured using a Nano-drop microvolume spectrophotometer. RNA was converted to cDNA using the High Capacity cDNA Reverse Transcription Kit (Applied Biosystems). cDNA was subsequently diluted (2.5 ng/µl) and added to DNA primers and FastStart Universal SYBR Green Master (Sigma-Aldrich, #4913850001). RT-PCR was performed on a Viia-7 Real-Time PCR System (Thermo-Fisher). Data is expressed using the ΔΔCT method with beta-2-microglobulin as a housekeeping gene.

Endothelial Cell Isolation

Mouse lungs were perfused with DPBS, minced, and digested with 3 mL Type 1 Collagenase (2 mg/ml in DPBS) at 37 degrees Celsius in a water bath for 1 hour. The samples were further homogenized using a #18 needle and subsequently filtered through a 40 μm cell strainer. Samples were subsequently centrifuged at 300 x g for 5 minutes, supernatant was removed, and pellets were washed with DPBS. Samples were centrifuged 300 x g, and pellets

were treated with red blood cell lysis buffer (Qiagen #158902). The sample was subsequently incubated with 5 μg anti-CD31 antibody (BD #553370) in 1 milliliter of DPBS and rotated at 4 degrees Celsius for one hour. Next, pre-washed 30 μl Dynabeads (Invitrogen #11035) were added to the cell sample and rotated at 4 degrees Celsius for an additional hour. Samples were subsequently washed and endothelial cells were harvested using magnetic separation.

Immunoblotting

Whole lungs were weighed and homogenized in 1 mL of DPBS followed by centrifugation at high speed (14,000 x g) for 5 minutes. The supernatant was removed and the pellet was incubated with 2% ODG buffer (previously described), sonicated, and incubated on a rotator for one hour at 4 degrees Celsius. The lysate was subsequently centrifuged at high speed (14,000 x g) for 10 minutes. The supernatant was removed and measured for protein concentration using Pierce BCA Protein Assay Kit (#23225).

Freshly isolated endothelial cells (4) were homogenized in RIPA buffer containing protease and phosphatase inhibitors. Protein concentration was quantified using Pierce BCA Protein Assay Kit (#23225). For studies involving cultured endothelial cells, dishes were washed twice with DPBS and lysed with 2% ODG buffer. Lysate was sonicated and centrifuged at 14,000 x g for 15 minutes. Protein concentration was measured as above for whole lung lysate and $CD31^+$ EC lysates and used for downstream western blot analysis.

Equal concentrations of protein were incubated with 4X Laemmli Sample Buffer (Biorad #1610747), heated at 95 degrees Celsius for five minutes, vortexed, and centrifuged at 14000 x g for five minutes. Samples were subsequently loaded on a 8-12% gel (previously described), separated via SDS-PAGE, transferred onto 0.45 micron nitrocellulose membranes (BioRad #1620115), and incubated in anti-PLVAP (NovusBio #NB100-77668), anti-VE-cadherin (Santa Cruz #sc-9989), and anti-Actin (BD Biosciences #612656) antibodies overnight. Membranes

were washed and incubated with secondary antibodies the next day, followed by detection with chemiluminescent reagents. Western blot quantification was performed using ImageJ software.

Statistics

Results were analyzed using GraphPad Prism Software. Student's t-test was used for experiments involving two experimental groups. One-way ANOVA with post-hoc Tukey's multiple comparison's test was used for experiments involving three or more experimental groups. Two-way ANOVA with repeated measures and post-hoc multiple comparisons test was used to compare basal weight change between genotypes over the indicated number of days.

Extended Data Figure and Table Legends

Figure E1. Validation of endothelial specific PV1 deletion in mice. Endothelial cells were isolated from controls and *PV1*$^{i\Delta EC}$ mice following two weeks after the final tamoxifen injection. Western blot analysis was used to verify PV1 deletion in the lungs; n=4 per group. Data are shown as mean ± SEM * $p < 0.05$.

Figure E2. Ascites in *PV1*$^{i\Delta EC}$ mice. Endothelial deletion of PV1 in adult mice induced rapid development of ascites, evidenced by fluid accumulation in the peritoneum of *PV1*$^{i\Delta EC}$ mice; n=3 per group.

Table E1. Composition of Ascites in *PV1*$^{i\Delta EC}$ mice. Ascites was collected from the peritoneum of *PV1*$^{i\Delta EC}$ mice and analyzed for biochemical content; n=3 per group

Figure E3. VE-cadherin (vascular endothelial cadherin) expression in *PV1*$^{i\Delta EC}$ mice. Whole lung lysates were isolated from controls and *PV1*$^{i\Delta EC}$ mice. Western blot analysis was used to determine VE-Cadherin expression; n=3 per group. Data are shown as mean ± SEM ($p=0.24$).

Figure E4: Endothelial PV1 deletion does not alter blood leukocyte number. Whole blood was withdrawn from the inferior vena cava of controls and *PV1*$^{i\Delta EC}$ mice. Data are shown as mean ± SEM; n=3 per group ($p > 0.05$)

Figure E5: Endothelial PV1 deletion does not increase mortality. Survival curves were plotted after observing control and *PV1*$^{i\Delta EC}$ mice post-tamoxifen for up to four months; n=3 per group.

Figure E6. Albumin permeability in multiple fenestrated organs. Endothelial PV1 deletion increased albumin permeability in fenestrated organs, as assessed by Albumin PS product in the (A) liver, (B) small Intestine, (C) large Intestine, and (D) kidneys; n=5-6 mice per group. Data are shown as mean ± SEM * $p < 0.05$.

Figure E7. Endothelial PV1 deletion does not disrupt lung epithelial cells or inter-endothelial junctional structure. At least 75 electron micrographs per group were used to determine whether epithelial cells were disrupted in *PV1*$^{i\Delta EC}$ mice and whether Au-albumin was present in endothelial junctions. (A) Micrographs showing alveoli from controls and *PV1*$^{i\Delta EC}$ mice, indicating the capillary lumen (Cap), endothelial cell (EC), and lung epithelial cells (AT1). Note the presence of edema in *PV1*$^{i\Delta EC}$ mice, indicated by asterisk (*) (scale bar, 0.5 μm). (B) Micrographs showing endothelial junctions (indicated by arrows) in controls and *PV1*$^{i\Delta EC}$ mice (scale bar, 0.2 μm). Loss of PV1 did not increase permeability via junctions in *PV1*$^{i\Delta EC}$ mice.

Figure E8. Endothelial PV1 deletion induces caveolae clustering. At least 75 electron micrographs per group were used to count the number of caveolae clusters in endothelial cells. (A) inset; Caveolae clusters indicated by arrowheads in inset (scale bar, 0.5 μm). (B) Quantification of caveolae cluster abundance in lung endothelium (scale bar, 0.2 μm). Experiments were performed with three mice per group. Data are shown as mean ± SEM ** $p < 0.01$.

Figure E9. Endotoxin reduces PV1 expression in mice. Endotoxin reduces endothelial PV1 expression in mice. Mouse lungs were harvested from mice following 4 days (1 hr/day) of either nebulized saline or LPS (lipopolysaachride). (A) Diagram depicting timeline of LPS treatment and lung collection. (B-C) PV1 protein levels determined by western blot; actin was used as a loading control. Quantification of PV1 expression was normalized to actin. Data are shown as mean ± SEM * $p < 0.05$. Panel A contains an illustration created with BioRender.com.

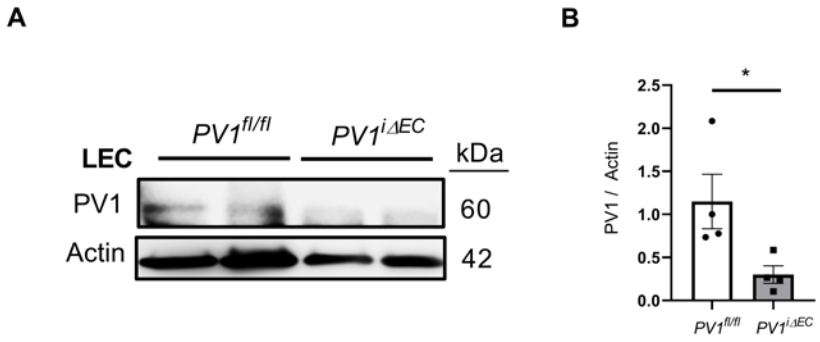

Figure E1. Validation of endothelial specific PV1 deletion in mice. Endothelial cells were isolated from controls and *PV1*$^{i\Delta EC}$ mice following two weeks after the final tamoxifen injection. Western blot analysis was used to verify PV1 deletion in the lungs; n=4 per group. Data are shown as mean ± SEM * $p < 0.05$.

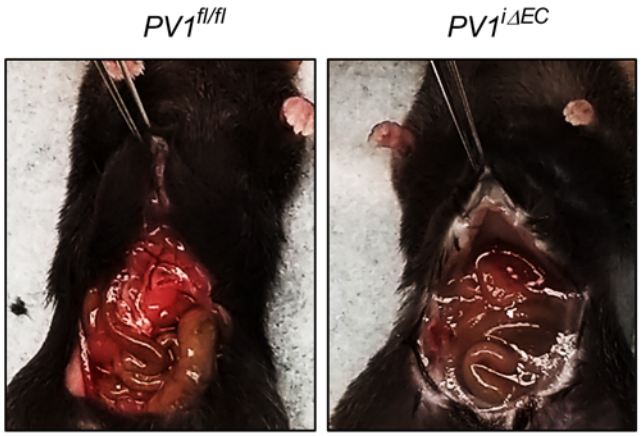

Figure E2. Ascites in *PV1$^{i\Delta EC}$* mice. Endothelial deletion of PV1 in adult mice induced rapid development of ascites, evidenced by fluid accumulation in the peritoneum of *PV1$^{i\Delta EC}$* mice; n=3 per group.

Ascites Fluid			
	Mean	SEM	N
Albumin (g/dL)	0.198	0.102	3
Total Protein (g/dL)	0.497	0.170	3
Alkaline Phosphatase (U/L)	6.667	1.202	3
Creatinine (mg/dL)	0.000	0.000	3
ALT (U/L)	4.000	0.577	3
AST (U/L)	20.667	6.667	3
BUN (mg/dL)	24.667	1.764	3
Glucose (mg/dL)	208.333	6.119	3
Cholesterol (mg/dL)	0.667	0.333	3
Triglcyeride (mg/dL)	17.667	1.764	3
Total Bilirubin (mg/dL)	0.010	0.006	3
Direct Bilirubin (mg/dL)	0.007	0.007	3
Calcium (mg/dL)	6.440	0.075	3
Sodium (mmol/L)	156.333	1.202	3
Potassium (mmol/L)	4.033	0.145	3
Chloride (mmol/L)	124.667	1.856	3

Table E1. Composition of Ascites in *PV1$^{i\Delta EC}$* mice. Ascites was collected from the peritoneum of *PV1$^{i\Delta EC}$* mice and analyzed for biochemical content; n=3 per group.

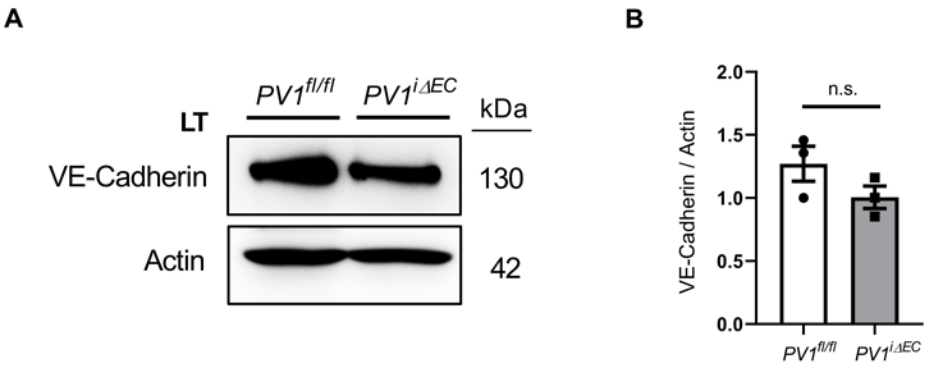

Figure E3. VE-cadherin (vascular endothelial cadherin) expression in *PV1$^{i\Delta EC}$* mice. Whole lung lysates were isolated from controls and *PV1$^{i\Delta EC}$* mice. Western blot analysis was used to determine VE-Cadherin expression; n=3 per group. Data are shown as mean ± SEM (p=0.17).

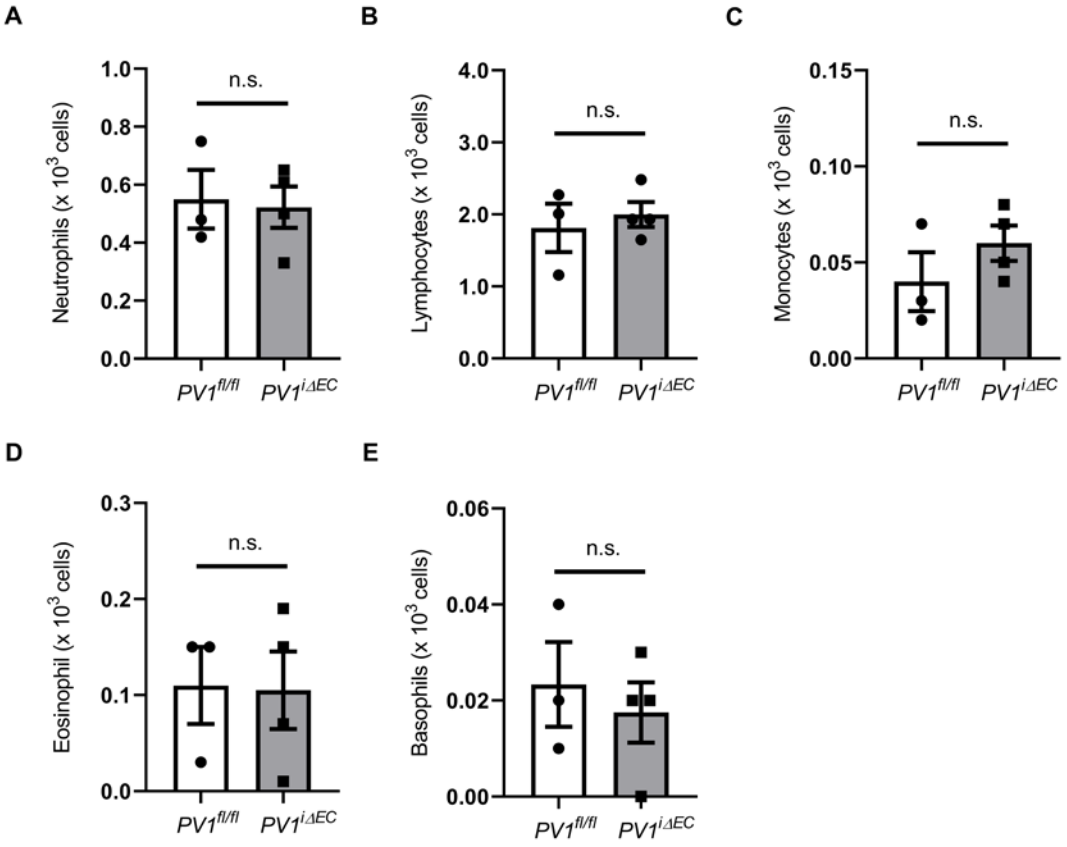

Figure E4: Endothelial specific PV1 deletion does not increase leukocyte numbers. Whole blood was withdrawn from the inferior vena cava of controls and *PV1*$^{i\Delta EC}$ mice. Data are shown as mean ± SEM; n=3 per group ($p > 0.05$).

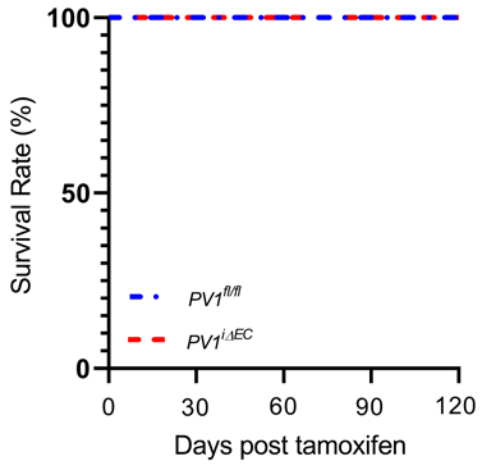

Figure E5: Endothelial PV1 deletion does not induce mortality. Survival curves were plotted using date from control and *PV1*$^{i\Delta EC}$ mice were observed post-tamoxifen for up to four months; n=3 per group.

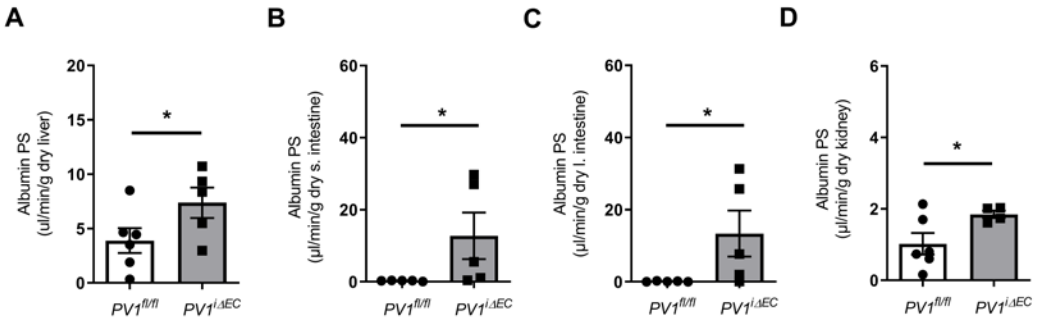

Figure E6. Endothelial albumin permeability in multiple fenestrated organs. Endothelial PV1 deletion increased albumin permeability in fenestrated organs, as assessed by Albumin PS product in the (A) liver, (B) small Intestine, (C) large Intestine, and (D) kidneys; n=5-6 mice per group. Data are shown as mean ± SEM * $p < 0.05$.

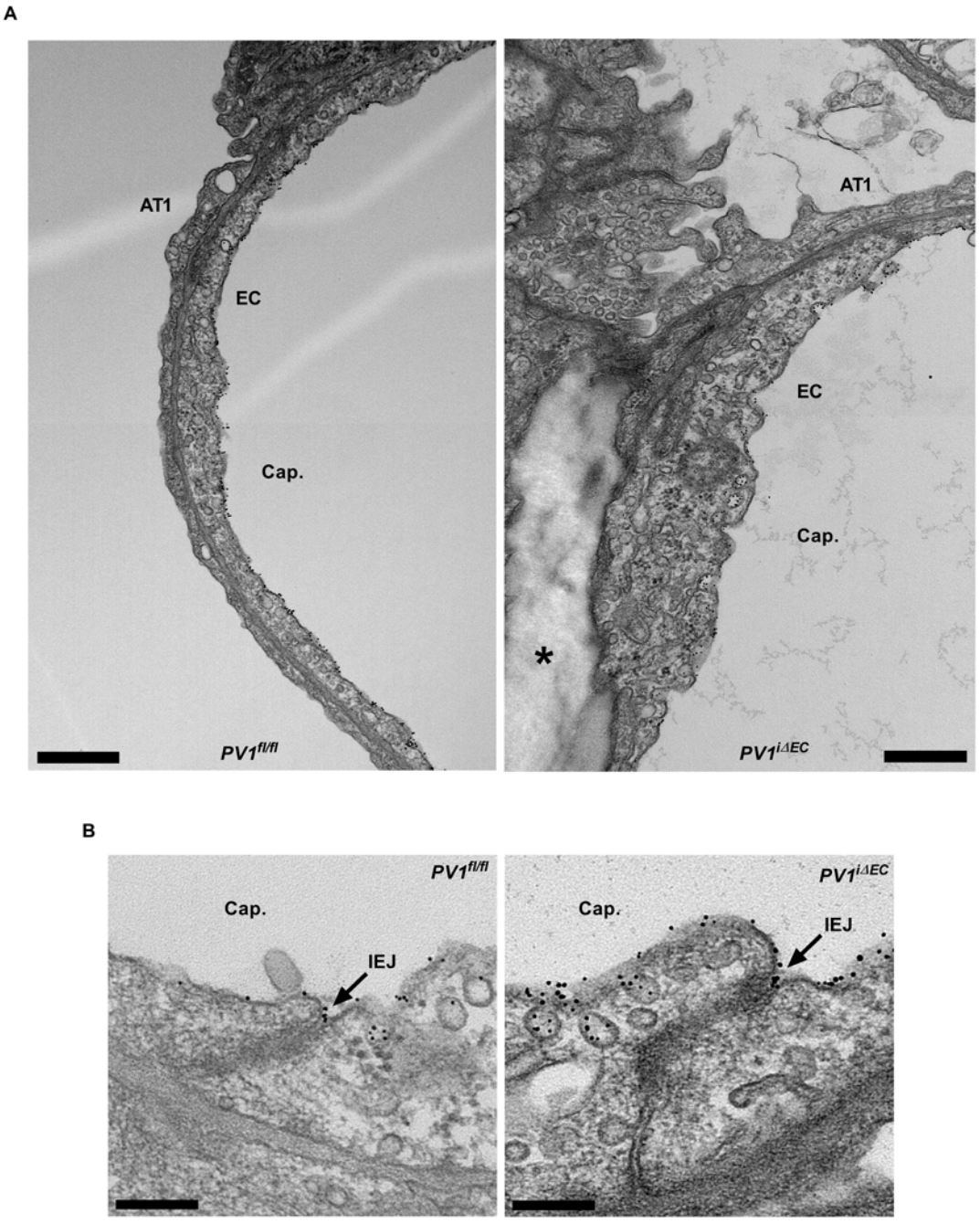

Figure E7. Endothelial PV1 deletion does not disrupt lung epithelial cells or inter-endothelial junction structure. At least 75 electron micrographs per group were used to determine whether epithelial cells were disrupted in *PV1*$^{i\Delta EC}$ mice and whether Au-albumin was present in endothelial junctions. (A) Micrographs showing alveoli from controls and *PV1*$^{i\Delta EC}$ mice, indicating the capillary lumen (Cap), endothelial cell (EC), and lung epithelial cells (AT1). Note the presence of edema in *PV1*$^{i\Delta EC}$ mice, indicated by asterisk (*) (scale bar, 0.5 μm). (B) Micrographs showing endothelial junctions (indicated by arrows) in controls and *PV1*$^{i\Delta EC}$ mice (scale bar, 0.2 μm). Loss of PV1 did not increase permeability via junctions in *PV1*$^{i\Delta EC}$ mice.

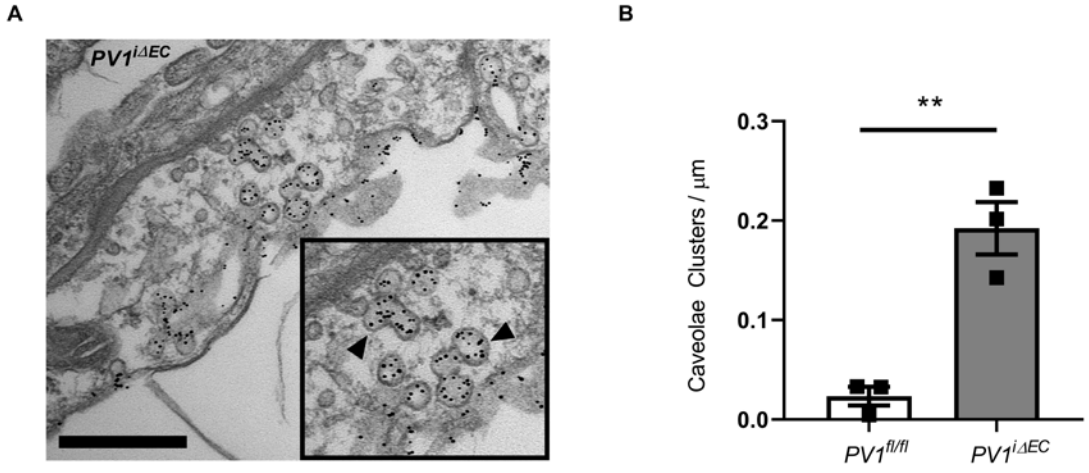

Figure E8. Endothelial PV1 deletion induces caveolae clustering. At least 75 electron micrographs per group were used to count the number of caveolae clusters in endothelial cells. (A) inset; Caveolae clusters indicated by arrowheads in inset (scale bar, 0.5 µm). (B) Quantification of caveolae cluster abundance in lung endothelium (scale bar, 0.2 µm). Experiments were performed with three mice per group. Data are shown as mean ± SEM ** $p < 0.01$.

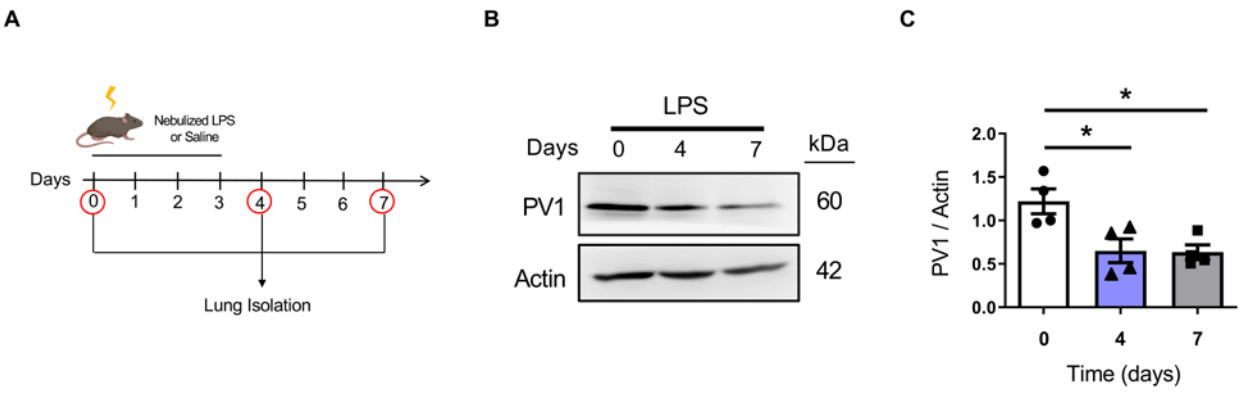

Figure E9. Endotoxin reduces endothelial PV1 expression in mice. Mouse lungs were harvested from mice following 4 days (1 hr/day) of either nebulized saline or LPS (lipopolysaachride). (A) Diagram depicting timeline of LPS treatment and lung collection. (B-C) PV1 protein levels determined by western blot; actin was used as a loading control. Quantification of PV1 expression was normalized to actin. Data are shown as mean ± SEM * $p < 0.05$. Panel A contains an illustration created with BioRender.com.

References

1. **Stan RV, Tse D, Deharvengt SJ, Smits NC, Xu Y, Luciano MR, McGarry CL, Buitendijk M, Nemani KV, Elgueta R, Kobayashi T, Shipman SL, Moodie KL, Daghlian CP, Ernst PA, Lee HK, Suriawinata AA, Schned AR, Longnecker DS, Fiering SN, Noelle RJ, Gimi B, Shworak NW and Carriere C.** The diaphragms of fenestrated endothelia: gatekeepers of vascular permeability and blood composition. *Dev.Cell.* 23: 6: 1203-1218, 2012.

2. **Piegeler T, Dull RO, Hu G, Castellon M, Chignalia AZ, Koshy RG, Votta-Velis EG, Borgeat A, Schwartz DE, Beck-Schimmer B and Minshall RD.** Ropivacaine attenuates endotoxin plus hyperinflation-mediated acute lung injury via inhibition of early-onset Src-dependent signaling. *BMC Anesthesiol.* 14: 57-2253-14-57. eCollection 2014, 2014.

3. **Friedrich EE, Hong Z, Xiong S, Zhong M, Di A, Rehman J, Komarova YA and Malik AB.** Endothelial cell Piezo1 mediates pressure-induced lung vascular hyperpermeability via disruption of adherens junctions. *Proc.Natl.Acad.Sci.U.S.A.* 116: 26: 12980-12985, 2019.

4. **Liu M, Zhang L, Marsboom G, Jambusaria A, Xiong S, Toth PT, Benevolenskaya EV, Rehman J and Malik AB.** Sox17 is required for endothelial regeneration following inflammation-induced vascular injury. *Nat.Commun.* 10: 1: 2126-019-10134-y, 2019.